# CFD THERMAL STUDIES OF THE AIR INSIDE THE STORAGE RING TUNNEL OF THE ALBA SYNCHROTRON LIGHT SOURCE FOR THE 3RD AND 4TH GENERATION DESIGNS

R. Galan Muñoz\*, Polytechnic University of Catalonia, Terrassa, Spain J. J. Casas, C. Colldelram, M. Quispe, ALBA-CELLS Synchrotron, Cerdanyola del Vallès, Spain

Abstract

The ALBA Synchrotron is currently designing its new version to become a  $4^{th}$  generation particle accelerator. In this new scenario, ALBA would produce a brighter and more coherent photon beam. As a result, during the analysis of matter, ALBA would provide capabilities hitherto inaccessible in terms of resolution, detection levels and understanding of chemical and electromagnetic properties. In this context, the thermal and geometric conditions inside the tunnel will be modified, in particular the Storage Ring will be completely new, while the other main parts such as the Booster Ring, the Transfer Lines, the Air Conditioning System and the tunnel itself will not be modified. The prediction of the thermal behaviour of the air inside the tunnel for the  $4^{th}$ generation case will be essential, considering that there is an influence of the stability of the air temperature inside the tunnel on the stability of the electron beam orbit. In this scenario, this work presents Computational Fluid Dynamics (CFD) studies of the air inside the current ALBA tunnel and for the development version of the  $4^{th}$  generation tunnel. Comparative studies of the temperature distribution in the air for both cases and proposals for the operation of the air conditioning system for the improvement of the thermal stability conditions of the air are presented. The studies are based on the FLUENT software of ANSYS WORKBENCH.

#### INTRODUCTION

In the field of synchrotron light sources, the stability of the electron orbit plays a crucial role in the production of photons to be used in the experimental lines. If it is not stable, the emitted light loses intensity and coherence. One of the factors that affects the stability of the electron orbit is the change in temperature of the air inside the tunnel [1] [2] [3].

In the case of the ALBA synchrotron ( $3^{rd}$  generation, ALBA I), after more than 13 years of operation, the global effects that affect the stability of the electron orbit have been under control. Currently, the ALBA Synchrotron divisions are working on redesigning the accelerator to become a  $4^{th}$  generation synchrotron (ALBA II) [4]. A complete modification of the Storage Ring will be conducted, while the other parts of the facility will remain equal. Therefore, the thermal distribution of the air in the tunnel will change.

CFD thermal simulations inside the tunnel of the ALBA Synchrotron have been performed to understand the air stratification within both generation designs. The commercial software ANSYS Fluent R.22.1 [5] has been used.

### **GEOMETRY**

Due to limited computational resources, the numerical studies have been performed in a reduced space of the tunnel, considering only two sectors of 14 as the volume under study, see Figure 1. The CAD simplified model features the Storage and Booster tunnel magnets and girders, external walls, air diffusers and both supplying and returning water pipes. The booster tunnel is the same for both designs and is composed of 100 magnets. However, the Storage Ring which will feature 720 magnets of distinct typologies in ALBA II compared to the 250 magnets that compose the present version (ALBA I).

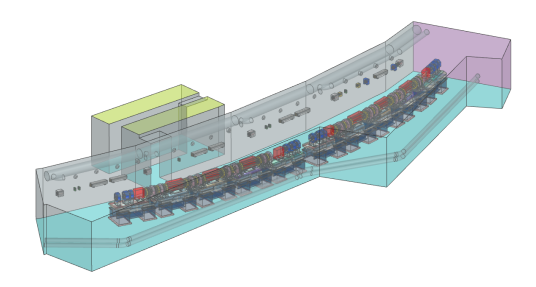


Figure 1:  $4^{th}$  Generation 2 sectors design.

# ALBA TUNNEL AIR CONDITIONING

The air-conditioning system of the ALBA tunnel uses a turbulent induction system with the aim of maintaining the most stable and constant thermal gradients possible. There are 4 air-conditioning units, each with a cooling capacity of 200~kW. The 4 units achieve a total airflow of  $54400~m^3/h$  and each one operates independently, controlling the temperature (set at  $23~^{\circ}C$ ) by varying the supply temperature from the diffusers ( $17~^{\circ}C$  to  $21~^{\circ}C$ ) and with a constant impulsion flow. A simplified diagram of an air-conditioning unit and its adjacent diffusers is shown in Fig. 2.

### ALBA TUNNEL CFD MODEL

For all the cases studied, the impulsion velocity of the air diffusers has been set to 9.694 m/s, a value extracted from the volumetric flow of the air-conditioning system. The air outlet is located on the outside of the chicane and two cases regarding the impulsion temperature are considered. In operating conditions, the temperature of the air diffusers is set to  $T_{inlet} = 17 \,^{\circ}C$  while on machine day  $T_{inlet} = 21 \,^{\circ}C$ . It is assumed that the sector under study is periodic, setting symmetrical boundary conditions on the side walls. The deionized water distribution pipes have been implemented

<sup>\*</sup> rosagalan1502@gmail.com

ISSN: 2673-5490

Figure 2: Individual unit of the air-conditioning system inside the ALBA tunnel.

in the model with temperatures set to  $T_s = 23 \,^{\circ}C$  and  $T_r =$ 25  $^{\circ}C$  for the supply and return pipes, respectively.

For the density of power dissipated from each magnet 2 scenarios have been studied: 5% and 10% of power dissipation. These values are presented in Tables 1, 2 and 3.

Table 1: Dissipated power in  $3^{rd}$  generation Storage Ring.

| Magnet   | 5% <b>Power</b> [W/m <sup>2</sup> ] | 10% <b>Power</b> [W/m <sup>2</sup> ] |
|----------|-------------------------------------|--------------------------------------|
| Quad 200 | 107.107                             | 214.215                              |
| Quad 260 | 109.003                             | 218.007                              |
| Quad 280 | 149.076                             | 298.152                              |
| Quad 500 | 172.241                             | 344.482                              |
| Sext 150 | 98.526                              | 197.053                              |
| Sext 220 | 86.550                              | 173.009                              |
| Bending  | 255.854                             | 511.709                              |

Table 2: Dissipated power in  $4^{th}$  generation Storage Ring.

| Magnet      | 5% <b>Power</b> $[W/m^2]$ | 10% <b>Power</b> $[W/m^2]$ |
|-------------|---------------------------|----------------------------|
| Quad 144 I  | 122.399                   | 244.798                    |
| Quad 144 II | 179.341                   | 358.682                    |
| Quad 239    | 132.947                   | 265.895                    |
| Quad 189    | 90.617                    | 181.233                    |
| Sextupole   | 86.466                    | 172.933                    |
| Octupole    | 1.234                     | 2.469                      |
| Bending     | 189.296                   | 378.592                    |

Table 3: Dissipated power in Booster Ring.

| Magnet     | 5% <b>Power</b> [W/m <sup>2</sup> ] | 10% <b>Power</b> [W/m <sup>2</sup> ] |
|------------|-------------------------------------|--------------------------------------|
| Quad 180   | 173.091                             | 346.183                              |
| Quad 340   | 66.425                              | 132.851                              |
| Sextupole  | 5.696                               | 11.391                               |
| Bending    | 127.177                             | 254.354                              |
| Correcting | 6.826                               | 13.653                               |

The simulations cases are assumed as 3D steady state with incompressible and turbulent flow as well as natural convection. The SST  $k - \omega$  turbulence model [6] and Coupled numerical scheme have been applied. A total of 8 cases

have been simulated, 4 cases for ALBA I (A1) and 4 cases for ALBA II (A2), combining the percentage of dissipated power by the magnets (PD) with the impulsion temperature of the air diffusers (TD). Table 4 summarizes the simulation cases and Fig. 3 presents outlines the boundary conditions.

Table 4: Simulation cases for ALBA I and ALBA II.

| Case       | % PD | TD [ºC] |
|------------|------|---------|
| A1-1; A2-1 | 5    | 17      |
| A1-2; A2-2 | 5    | 21      |
| A1-3; A2-3 | 10   | 17      |
| A1-4; A2-4 | 10   | 21      |

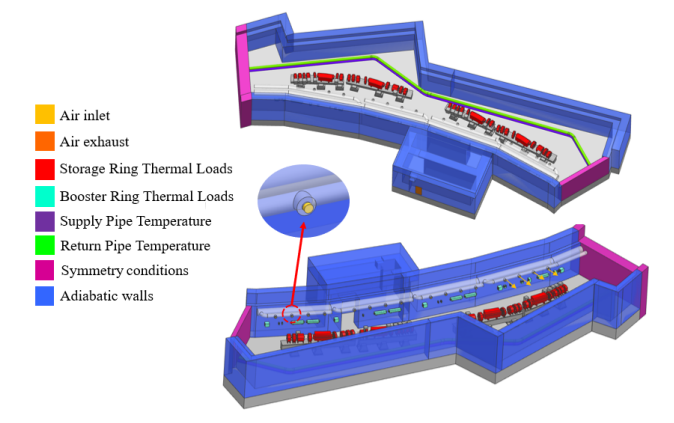


Figure 3: Summary of boundary conditions in  $3^{rd}$  generation design.

### **MESH GENERATION**

Mesh studies have been performed to find a balance between the necessary refinements, specifically in the outlet of the air diffusers and the coils of the magnets (see Figure 4), and the computational resources. Asymptotic results are obtained for 20 million of elements for ALBA I and 32 million for ALBA II, approximately. A general element size of 100 mm has been considered, with refinements of 5 mm in the previously mentioned zones.

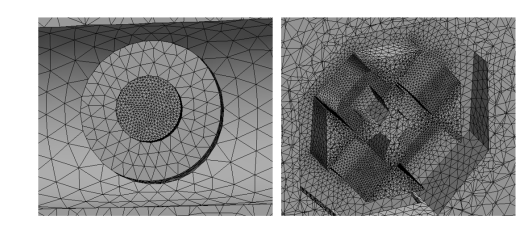


Figure 4: Grids near inlet and magnet coils.

Ontent from this work may be used under the terms of the CC BY 4.0 licence (© 2025). Any distribution of this work must maintain attribution to the author(s), title of the work, publisher, and DOI

ISSN: 2673-5490

Temperature distributions have been studied in 3 horizontal lines of 1.1 m length, located in the central area of the air volume. These Upper, Middle and Lower lines are positioned at 2.68, 2.27 and 1.86 m above ground level, respectively (see Fig. 5).

RESULTS AND DISCUSSION

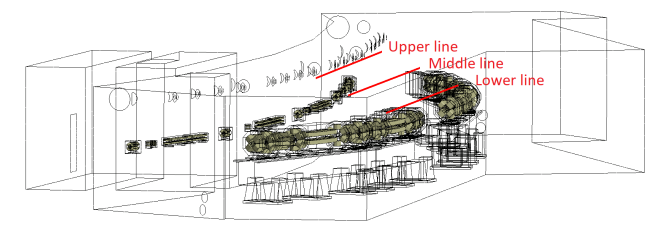


Figure 5: Details of the 3 lines considered for the study of air temperature distribution in the tunnel.

Figure 6 compares both generation cases when the power dissipation in the magnets is 5% and the air conditioning injection temperature is 17 °C. For all three study lines, the temperature distribution values for ALBA I are higher than those for ALBA II. It is worth highlighting that the temperature distribution in the lower line is considerably more uniform in the case of ALBA II, while ALBA I exhibits very pronounced temperature peaks.

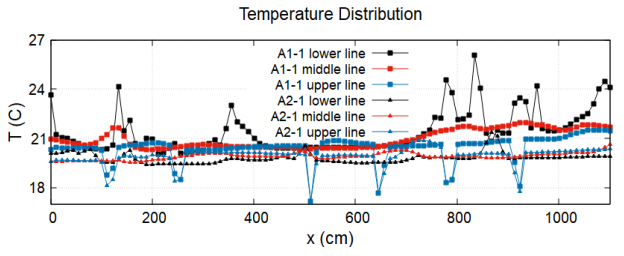


Figure 6: Comparison of temperature between  $3^{rd}$  and  $4^{th}$  generation for cases A1-1 and A2-1.

The temperature values for the power dissipation cases of 5% vs. 10% in ALBA I are presented in Fig. 7 . It is observed that the air is warmer in the case of 10% of dissipation, in orders of magnitude between 2 °C and 3 °C.

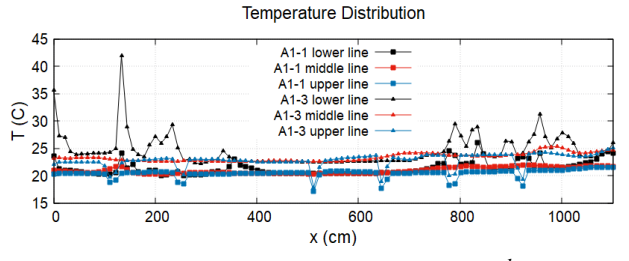


Figure 7: Comparison of temperature in the  $3^{rd}$  generation design for cases A1-1 and A1-3.

Figure 8 shows contours of temperature on a horizontal plane located at the height of the diffusers for the case A2-4.

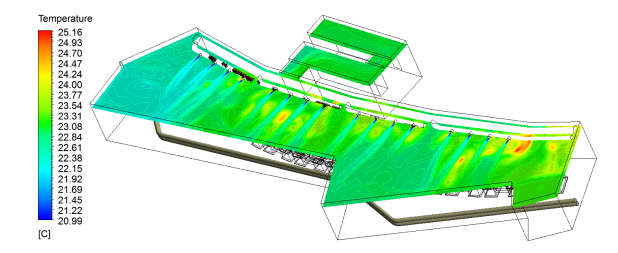


Figure 8: Temperature distribution for the case A2-4.

Figure 9 shows the temperature distribution in a XZ plane located at 2 m for ALBA I for the case A1-4. This scenario is the worse case: highest impulsion temperature from the air diffusers and a 10% of dissipated power. It is clear that greater values of temperature are near Storage Ring magnets.

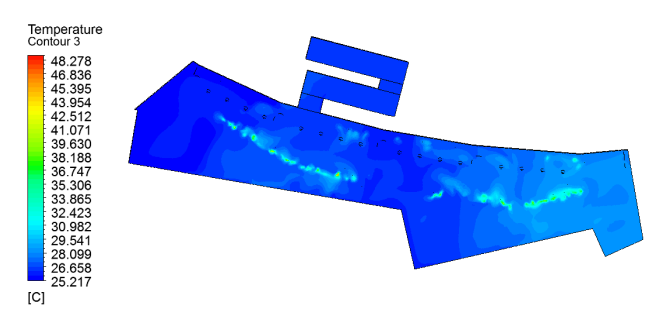


Figure 9: Temperature distribution for the case A1-4.

The distribution of the velocity map maintains similar patterns of behaviour among all cases (Fig. 10), which indicates that the effect of forced convection is predominant compared to that of natural convection.

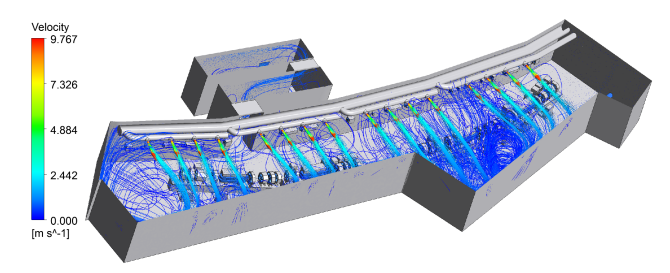


Figure 10: Velocity distribution for the case A1-2.

## CONCLUSION AND FUTURE WORK

The basis for comprehending the air stratification inside the tunnel of the ALBA Synchrotron has been established. Based on the results obtained, it can be concluded that the future modification of the Storage Ring - which should be noted that is not yet final - will not significantly affect the air temperature distribution within the tunnel in its central zone. Future work featuring more detailed geometries, other heat sources such as cable trays or vacuum pumps and variations of the inlet discharge angle as well as transient studies are key to validate the CFD model. A detailed research on the

Content from this work may be used under the terms of the CC BY 4.0 licence (© 2025). Any distribution of this work must maintain attribution to the author(s), title of the work, publisher, and DO

thermal behaviour of the air in the spaces between the 4<sup>th</sup> generation magnets and in the magnet bodies themselves would be interesting since the separation between the magnets is very small compared to the case of ALBA I.

# **ACKNOWLEDGMENTS**

Authors would like to thank our colleagues at the ALBA Synchrotron, Valentí Massana Gràcia and Gabriel Peña, for their valuable contributions to this work.

### REFERENCES

- [1] L. Emer, "Measurement of Thermal Effects on the Advanced Photon Source Storage Ring Vacuum Chamber", in 2001 Particle Accelerator Conference, in PAC-01, vol. 2. IEEE, pp. 1276–1278.
  - doi:10.1109/pac.2001.986652.

- [2] C. R. Chen *et al.*, "The Correlation between the Beam Orbit Stability and the Utilities at SRRC", in *Proc. EPAC'98*, Stockholm, Sweden, Jun. 1998, paper TUP38C, pp. 2309–2311.
- [3] J.-C. Chang, J.-R. Chen, Y.-C. Chung, M. Ke, C. Y. Liu, and Z.-D. Tsai, "Numerical Simulation and Air Conditioning System Study for the Storage Ring of TLS", in *Proc. IPAC'10*, Kyoto, Japan, May 2010, paper THPEB075, pp. 4041–4043.
- [4] C. Biscari, E. Aigner, K. Attenkofer, J. Casas, S. Ferrer, O. Matilla, J. Nicolas, R. Pascual, F. Pérez, M. Pont and A. Sánchez, "ALBA Synchrotron Heading Towards Its Upgrade", Synchrotron Radiat. News, vol. 37, no. 1, pp. 18–23, Jan. 2024. doi:10.1080/08940886.2024.2312056
- [5] ANSYS. Fluent product documentation, https://www.ansys.com
- [6] F.R. Menter, R. Lechner, A. Matyushenko, "Best Practice: RANS Turbulence Modeling in Ansys CFD", Ansys, 2023